RSC Advances

PAPER

View Article Online
View Journal | View Issue



Cite this: *RSC Adv.*, 2025, **15**, 11826

# Fabrication of robust polyimide-coated solid phase microextraction fibers for efficient extraction of fifteen polycyclic aromatic hydrocarbons from environmental water†

Aiying Song, *[a] Rong Liu,[a] Xinghe He[a] and Linlin Wei*[b]

A novel supporting material was developed by pulling melted glass onto stainless steel, providing a mechanically robust and chemically stable substrate. A polyimide-coated fiber for solid-phase microextraction (SPME) was then fabricated using a simple dipping method. The strong interactions between the polyimide coating and analytes, attributed to abundant unshared electron pairs in the p orbitals of O and N atoms, as well as π electrons in the C=O bond and benzene ring, contributed to the high extraction efficiency for sixteen polycyclic aromatic hydrocarbons. The developed polyimide-coated fiber-based SPME method, coupled with gas chromatography-flame ionization detection, exhibited low limits of detection (0.11–1.23 μg $L^{-1}$) and a wide linear range (1–500 μg $L^{-1}$) for polycyclic aromatic hydrocarbons in water samples. The method demonstrated excellent repeatability, with single-fiber repeatability ranging from 2.9% to 6.9% and fiber-to-fiber reproducibility between 3.9% and 11.5%. The recoveries of the analytes were between 82.7% and 107.2%. Additionally, the fiber exhibited outstanding durability, maintaining its extraction performance after more than 150 uses. The developed method was successfully applied for the determination of polycyclic aromatic hydrocarbons in river, pond, and sewage water samples, highlighting its potential as a sensitive, reliable, and cost-effective tool for environmental analysis.

Received 16th January 2025
Accepted 9th April 2025

DOI: 10.1039/d5ra00390c

rsc.li/rsc-advances



## 1. Introduction

Solid-phase microextraction (SPME) is an efficient sample preparation method in chemical analysis that integrates sampling, extraction, preconcentration, matrix removal, and gas chromatograph (GC) introduction. It collects analytes from various samples, isolates them on a coated fiber without the use of solvents, enhances detection sensitivity, eliminates unwanted substances, and transfers them to a GC for analysis.[1,2] Its simplicity, solvent-free nature, selectivity, and flexibility have made SPME a popular alternative to traditional sampling methods, with widespread applications in fields such as food analysis, botany, clinical studies, pharmaceuticals, forensics, and environmental monitoring.[3–8] The fiber used in SPME is a critical component that determines extraction performance, including selectivity, capacity, and longevity. Typically, SPME fibers consist of a coating material supported by a substrate, although substrateless fibers are also an option. Numerous coating materials have been developed, with commercial options such as polydimethylsiloxane (PDMS), polyacrylate (PA), divinylbenzene (DVB), carboxen (CAR), carbowax (CW), and their combinations.[9] These coatings cater to diverse applications due to their varying polarities and properties. However, they have limitations, including restricted operational temperatures, limited selectivity and robustness, solvent swelling, carryover issues, and high costs. These drawbacks have driven researchers to explore alternative SPME coatings.

Recent advancements in material chemistry have enabled the creation of innovative sorbents with customized morphologies and physicochemical properties, expanding their applicability in diverse SPME techniques. Emerging coating materials include carbon nanotubes,[10–12] graphitic carbon nitride,[13] graphene,[14] reduced graphene oxide,[15] boron nitride,[16] ionic liquids,[17] metal–organic frameworks,[18] molecularly imprinted polymers,[19] and covalent organic frameworks.[20,21] The extraction performance of these materials depends on their morphology and physicochemical characteristics. A key guiding principle in the development of coating materials is "like dissolves like," where increasing the surface area and thickness or length of the coatings can further enhance their extraction efficiency. Regarding supporting materials, stainless steel wire

[a]School of Judicial Police (Public Security), Gansu University of Political Science and Law, No. 6, Anning West Road, Anning District, Lanzhou, 730070, PR China. E-mail: 58250329@qq.com

[b]Toxicological Laboratory, Gansu Provincial Center for Disease Control and Prevention, Lanzhou 730020, China. E-mail: 908830476@qq.com

† Electronic supplementary information (ESI) available. See DOI: https://doi.org/10.1039/d5ra00390c

(SSW) and silica fiber are commonly employed. SSW offers excellent mechanical strength and thermal stability but has an inert surface, complicating chemical bonding for coating. Silica, with its abundant surface Si–OH groups, facilitates strong chemical bonding but is fragile, significantly limiting its lifespan. Additionally, silica-based fibers typically have coating lengths restricted to 1 cm due to their fragility. Therefore, developing a supporting material that combines the merits of SSW and silica fiber is a priority in SPME research.

Polyimide (PI), an organic polymer with a stiff aromatic backbone, demonstrates excellent thermal and chemical stability, solvent resistance, and mechanical strength.[22] These properties, along with its rich chemical groups, have made PI a viable extraction material, utilized in various forms such as electrospun nanofiber membranes,[23] magnetic mesoporous composites,[24] phase transformation coatings,[25] and porous particles.[26] PI has shown affinities for compounds like estrogens,[27] Sudan dyes,[28] rhodamine B,[24] polycyclic aromatic hydrocarbons (PAHs),[29] parabens,[30] and chromium trifluoroacetylacetonate ($Cr(tfa)_3$).[31] Its stable chemical and physical properties, along with its ability to absorb both polar and nonpolar compounds, make PI an ideal material for SPME coatings. However, studies on PI-coated SPME fibers remain limited. PAHs are ubiquitous environmental contaminants produced during incomplete combustion or industrial processes. Due to their toxicity and potential mutagenic, teratogenic, and carcinogenic effects, analyzing trace levels of PAHs in various matrices has been extensively studied.[32–34] To address these challenges, we developed a novel supporting material by pulling melted glass onto stainless steel, combining the mechanical strength of stainless steel wire with the chemical properties of glass. Polyimide-coated fibers were then fabricated using a simple dipping method. The PI coating exhibited a high affinity for electron-rich PAHs (the physicochemical properties of the analytes are shown in Table S1†) due to the presence of abundant unshared electron pairs in the p orbitals of oxygen and nitrogen atoms, as well as $\pi$ electrons in the C=O bond and benzene ring. By coupling GC-FID, we established an SPME/GC-FID method for the sensitive detection of trace levels of PAHs in environmental water samples.

# 2. Experimental

## 2.1. Reagents and materials

Polyimide (PI) was obtained from Sujia Polymer Material Co., Ltd (Dongguan, Guangzhou, China). A standard solution of PAHs containing NAP, ACY, FLU, PHE, ANT, FLA, PYR, BaA, BaF, BbF, BkF, BaP, IcdP, DahA, and CHR at a concentration of 200 μg $L^{-1}$ was purchased from O2si Smart Solutions (Charleston, South Carolina, USA). The solution was stored at −20 °C until use. Working standard solutions were freshly prepared each day by appropriate dilution with acetonitrile. Sodium chloride was procured from Chengdu Cologne Chemical Co., Ltd (Chengdu, China), while deionized water was produced using a Milli-Q ultrapure water system (Millipore, Elix5, and Milli-Q). SSW (0.15 mm outer diameter) was obtained from Baofeng Metal Material Company (Shenzhen, China) and cut into 3 cm sections for fiber preparation. Glass capillaries (0.3 mm inner diameter) were sourced from Donghai Jingao Glass Products Co., Ltd (Lianyungang, China). The SPME device was purchased from Supelco (Bellefonte, PA, USA).

## 2.2. Instruments

Scanning electron micrographs (SEM) and electron dispersive spectroscopy (EDS) of the SPME fiber coatings were obtained using a Shimadzu SS-550 scanning electron microscope (Hitachi SU8020, Japan) operating at 20.0 kV. Separation of PAHs was carried out using an Agilent 8890 gas chromatograph (GC; Agilent, Shanghai, China) equipped with an HP-5 capillary column (30 m × 0.32 mm i.d., 0.25 μm film thickness), a flame ionization detector (FID), and a split/splitless injection port. For PAH detection, the injection port temperature was set to 300 °C in splitless mode, while the FID temperature was maintained at 330 °C. Nitrogen gas (purity 99.99%) was used as the carrier gas at a flow rate of 2.0 mL $min^{-1}$, with air and hydrogen flow rates set at 400 mL $min^{-1}$ and 30 mL $min^{-1}$, respectively. The GC oven program was set to an initial temperature of 100 °C, ramped to 310 °C at 5 °C $min^{-1}$, and held for 1 min, resulting in a total run time of 42 min.

## 2.3. Preparation of PI-coated fiber

The fabrication of the polyimide (PI)-coated fiber involved several sequential steps, as shown in Fig. 1. A stainless steel wire (SSW) with an outer diameter of 0.15 mm was cut into 5 cm-long segments, which were carefully cleaned by wiping with filter paper. One cleaned SSW segment was then inserted into a 3 cm-long glass capillary with an inner diameter of 0.3 mm. The glass capillary was held at both ends, and its middle part was heated using a butane flame. To ensure even heating, the glass capillary was rotated during the heating process. Once the glass capillary became red-hot and softened, the left tip of the glass capillary and the SSW were held stationary, while the right tip was slowly pulled to form a thin, uniform coating, thus creating the desired supporting material. Next, 1 mL of PI was placed into a 1.2 mL vial to form a PI column with a height greater than 2 cm. The aforementioned supporting material was then inserted into the PI column through a 0.50 mm hole located in the center of the cap septum. After fully immersing the supporting material in the PI, it was gradually pulled vertically through the hole. This process removed excess PI from the supporting material and ensured uniform adhesion of the PI coating. The freshly coated supporting material was subsequently dried at 100 °C and 150 °C for 2 h each, ensuring that the PI coating was firmly fixed onto the supporting material. The coating process was repeated three times to achieve a homogeneous coating with a thickness of approximately 20 μm. Finally, the prepared fiber was mounted onto the SPME holder and conditioned in the GC injection port at 280 °C until a stable baseline was achieved, a process that took approximately 2 h.

## 2.4. SPME procedures

For the direct immersion SPME procedure, 25 mL of either standard PAH working solutions (100 μg $L^{-1}$) or environmental

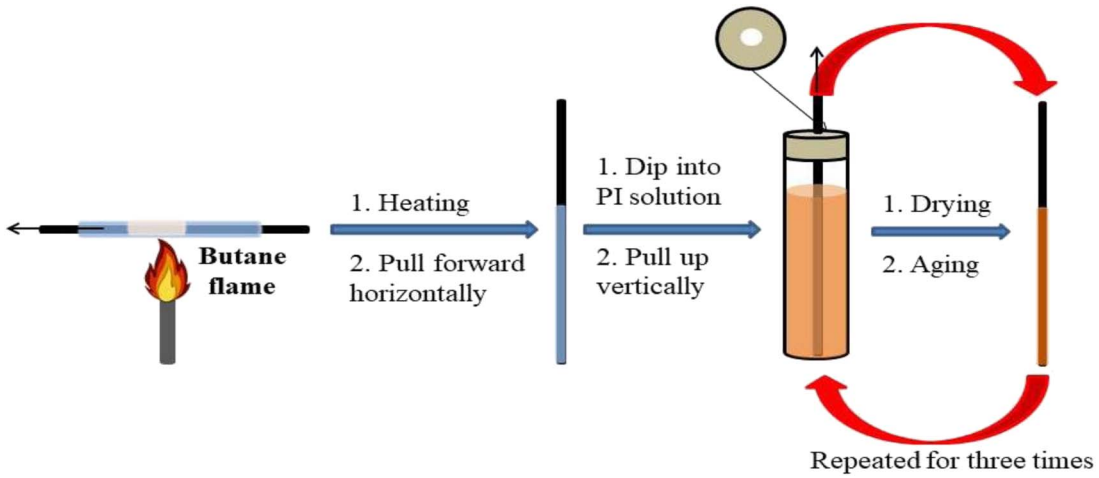


Fig. 1 Schematic demonstrating of the fabrication processes of FI-coated SPME fiber.

water samples were placed into a 40 mL glass vial. A Teflon-coated stir bar and 7.5 g of sodium chloride were added, and the vial was sealed with a PTFE-coated septum. The extraction temperature was maintained at 80 °C using a thermostatic water bath, with magnetic stirring set at 500 rpm to ensure thorough agitation. The SPME fiber was carefully inserted into the vial's headspace and exposed for 40 min to allow adsorption equilibrium of the target PAHs onto the fiber coating. After the extraction step, the fiber was retracted into the needle sleeve and introduced into the GC injection port for analyte desorption at 280 °C for 5 min. Before commencing the next extraction–desorption cycle, the fiber was conditioned in the injection port at 280 °C for 5 min to remove any residual compounds, ensuring consistent performance across multiple runs.

# 3. Results and discussion

## 3.1. The reason for choosing PI as coating material

We chose the PI as the SPME coating material because its following advantages: first, PI exhibits exceptional solvent and thermal stability, which extends the lifespan of PI-coated fibers. Second, PI contains abundant unshared electron pairs in the p orbitals of oxygen and nitrogen atoms, as well as π electrons in the C=O bond and benzene ring. This structure gives it a high affinity for electron-rich compounds (*e.g.*, PAHs) through π–π and/or p–π stacking interactions.

## 3.2. PI coating for enhanced mechanical strength

PI can be readily applied to silica capillary, significantly improving their mechanical strength. This is why PI is commonly used as a coating for chromatography capillary columns. However, the thin structure of SPME fibers and the bare exposure of their rear tips make them vulnerable to breakage during extraction procedures. While SSW offers excellent mechanical strength, achieving a uniform PI coating on SSW alone is difficult. To address this limitation, a hybrid supporting material was created by heating and pulling glass onto SSW (details provided in Section 2.3), forming a thin glass layer around the wire. A PI coating was then applied to the prepared supporting material using a sequence of dipping, drying, and aging steps. The inclusion of SSW substantially enhanced the fiber's mechanical strength and allowed for an extended coating length. For optimal extraction capacity and ease of use, the fiber length was set at 2 cm in this study.

## 3.3. Characterization of the PI-coated fiber

SEM images of the supporting material and PI-coated fiber are shown in Fig. 2. The low-magnification image of the supporting material (Fig. 2a and S1a†) demonstrates that the glass layer was uniformly and smoothly distributed along the stainless steel wire, giving the glass layer a sleek appearance. The EDX spectrum (Fig. S1b†) of the supporting material showed the predominant presence of O and Si atoms, with weight percentages of 53.21% and 27.93%, respectively. In addition, C, Na, Al, K, Ca, and Ba atoms were also detected in the glass coating layer, likely originating from the glass composition, with a total weight percentage of 18.86%. The high-magnification cross-sectional image (Fig. 2b) reveals that the glass layer closely adhered to the SSW, with a thickness of approximately 20 μm. As seen in Fig. 2a and S1c,† the surface becomes rougher but remains uniform after coating the PI onto the glass layer. The EDX spectrum of the PI-coated fiber (Fig. S1d†) revealed the presence of C, N, and O atoms, with weight percentages of 70.29%, 0.15%, and 29.56%, respectively. These results are generally consistent with the composition of PI. The cross-sectional view of the fiber (Fig. 2b) clearly shows the SSW located at the center of the fiber, with the PI coating tightly wrapped around the glass layer. The thicknesses of the glass layer and the PI coating were approximately 20 μm and 10 μm, respectively. These findings validate the effectiveness of the proposed method for fabricating both the supporting material and the PI-coated fibers.

## 3.4. Affinity of PI coating for PAHs

The structure of PI includes various types of electrons, such as lone pairs in the p orbitals of oxygen and nitrogen atoms, as well

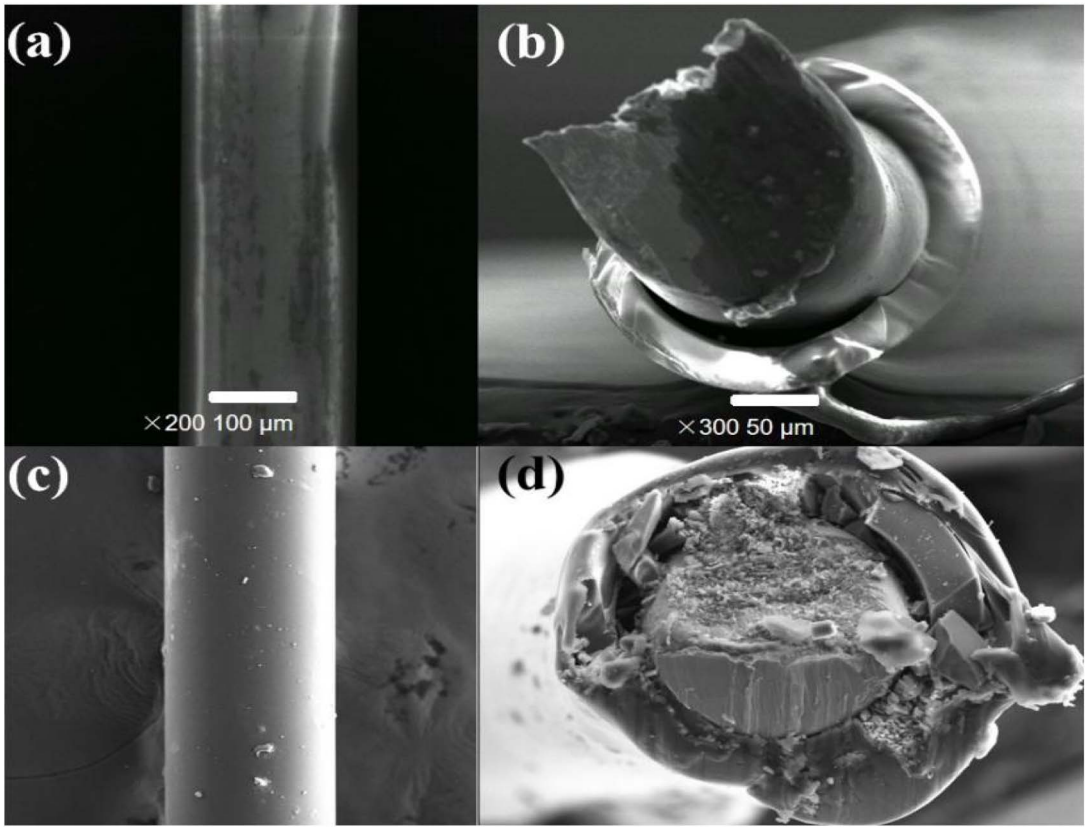


Fig. 2 SEM image (a) and cross-sectional view (b) of the supporting material; SEM image (c) and cross-sectional view (d) of the PI-coated fiber.

as π electrons in C═O bonds and benzene rings. This electronic configuration allows the PI coating to exhibit strong affinity for polycyclic aromatic hydrocarbons (PAHs) through p–π conjugate interactions and π–π stacking interactions.[35] These multiple interaction mechanisms give PI coatings a significantly higher affinity for a broader range of PAH compounds compared to other materials, such as graphene (*e.g.*, NAP, ACY, FLU, PHE, ANT, FLA),[36] reduced graphene oxides (*e.g.*, NAP, ACY, FLU, PHE, ANT, FLA, PYR, B[*b*]F), and COF@$Ti_3C_2T_x$ (*e.g.*, ACY, FLU, PHE, ANT, PYR).[37,38] This distinctive property makes PI an excellent choice for PAH extraction.

### 3.5. Stability of PI-coated fiber

The solvent and thermal stability, as well as mechanical strength of an SPME fiber are critical factors for its performance and longevity. To evaluate the stability of the PI-coated fiber, it was immersed for 1 h in different solvents typically encountered during extractions: 0.1 mol per L HCl solution, 0.1 mol per L NaOH solution, and 1 mol per L methanol. After immersion, the fiber was thoroughly rinsed with deionized water and dried at 150 °C for 30 min; to assess its thermal stability, the PI-coated fiber was conditioned at temperatures of 290, 300, and 310 °C for 30 min. Subsequently, the fiber's extraction efficiency for PAHs was evaluated. The ratios (*r*) of the extraction efficiency after *versus* before solvent and thermal treatment are presented in Table S1,† with values ranging from 0.84 to 1.02. These results indicate that the fiber's extraction performance remained consistent, demonstrating strong solvent resistance and excellent thermal stability up to 310 °C. The mechanical strength of the fiber was evaluated after 150 extraction cycles. The extraction efficiency was also measured, and the corresponding *r* values (Table 2) ranged from 0.87 to 0.95, indicating minimal change in performance even after repeated use. This robustness can be attributed to the high mechanical strength of the PI coating and the glass-modified SSW core, ensuring durability for over 150 extractions.

### 3.6. Choice of extraction mode

In preliminary experiments, it was observed that IPY, DBA, and BPE could not be effectively extracted using the headspace mode, likely due to their high boiling points, which hinder volatilization into the headspace (the boiling points of all analytes are listed in Table S1†). To enable comprehensive extraction of all target PAHs (sixteen analytes), the direct immersion (DI) extraction mode was therefore selected for this study.

### 3.7. Optimization of SPME conditions

To achieve satisfactory extraction efficiency and sensitivity, various experimental factors, including extraction time, stirring speed, salt concentration, desorption temperature, and desorption time, were investigated. The experimental details

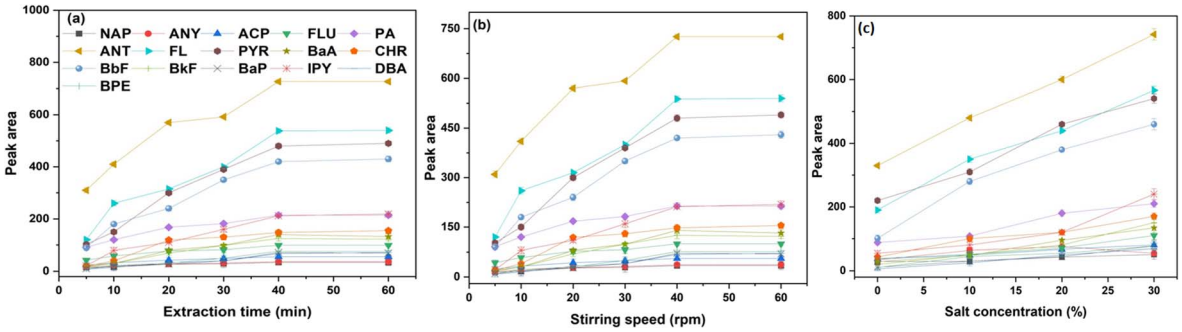


Fig. 3 Effect of the experimental conditions on the extraction efficiency of PI-coated fiber for 100 μg $L^{-1}$ PAHs, including (a) extraction time, (b) stirring speed, and (c) salt concentration. Errors bars show the standard deviation of the mean ($n = 3$).

are shown in Fig. 3. Optimization experiments were conducted using 25 mL of water spiked with 100.0 μg $L^{-1}$ of PAHs, with each condition tested in triplicate to ensure reliability.

**3.7.1. Extraction time.** The duration of extraction influences the equilibrium among analytes in the sample, headspace, and fiber coating. Extraction times ranging from 5 to 60 min were tested. As shown in Fig. 3a, the signal responses for the fifteen PAHs increased significantly with longer extraction times, plateauing between 40 and 60 min, indicating that adsorption equilibrium was achieved at 40 min. Consequently, 40 min was selected as the optimal extraction time for further analyses.

**3.7.2. Stirring speed.** Stirring facilitates the diffusion of analytes from the solution to the headspace and subsequently onto the fiber coating, thereby enhancing extraction efficiency. To determine the optimal stirring speed, rates ranging from 0 to 700 rpm were evaluated. As depicted in Fig. 3b, maximum extraction efficiency was achieved at a stirring speed of 500 rpm. At higher speeds, the solution occasionally splashed onto the surface of the fiber, reducing extraction efficiency and compromising repeatability. Consequently, 500 rpm was selected as the optimal stirring speed for further analyses.

**3.7.3. Ionic strength.** Ionic strength influences the distribution constant of analytes, particularly nonpolar compounds, between the headspace and the sample solution, thereby affecting extraction efficiency. Sodium chloride (NaCl) concentrations ranging from 0% to 30% (w/v) were tested. As shown in Fig. 3c, extraction efficiency was the highest at a NaCl concentration of 30%, beyond which efficiency declined due to increased sample viscosity. Accordingly, a concentration of 30% NaCl was selected for subsequent experiments.

**3.7.4. Desorption temperature and time.** Desorption temperature is critical for the complete release of analytes from the fiber coating without compromising its integrity. Temperatures ranging from 260 to 290 °C were evaluated, with Fig. S2† showing the highest extraction efficiency at 280 °C. Temperatures above 280 °C did not significantly improve performance. Thus, 280 °C was selected as the optimal desorption temperature. Desorption time also affects analyte recovery and minimizes cross-contamination. Times between 1 and 9 min were tested, with Fig. S3† showing a plateau in peak areas after 5 min. Therefore, a desorption time of 5 min was chosen for further analyses. Accordingly, the conditions for the HS-SPME of PHCs were established as follows: extraction time, 40 min; stirring speed, 500 rpm; salt (NaCl) concentration, 30% (w/v); desorption temperature, 280 °C; and desorption time, 5 min.

### 3.8. Comparison of PI-coated fiber with commercial PDMS fiber

The overall extraction performance of the PI-coated fiber was evaluated in comparison with a commercial 100 μm PDMS fiber, which is recognized as one of the most effective materials for PAH enrichment due to its inherently nonpolar polymer composition. Given the difference in coating thickness and length between the fibers, the extraction time profile of the PDMS fiber was examined to ensure that the comparison was made under equilibrium conditions. The findings revealed that the PDMS fiber reached equilibrium within 50 min for extracting the eight PAHs. Accordingly, 50 min was determined as the optimal extraction time for the commercial fiber. The performance of the PI-coated fiber was further compared to that of the commercial fiber for DI-SPME of a 100 μg per L PAH solution, with each fiber operated under its respective optimal conditions. The comparison was based on the extraction efficiency of

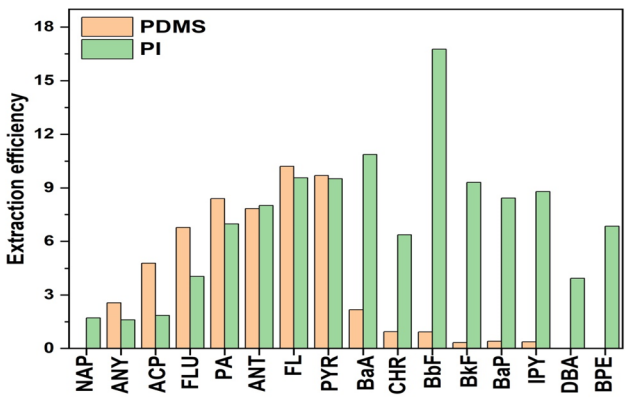


Fig. 4 Comparison between PDMS and PI coating: extraction efficiency toward sixteen PAHs.

Table 1 Analytical performance for GC/FID determination of PAHs using PI-coated fiber

| Compound | Linear range ($\mu g\ L^{-1}$) | $R^2$ | Detection limit ($\mu g\ L^{-1}$) | RSD | |
|---|---|---|---|---|---|
| | | | | One fiber (%, $n = 5$) | Fiber-to-fiber (%, $n = 3$) |
| NAP | 10–500 | 0.994 | 1.23 | 3.9 | 9.2 |
| ANY | 10–500 | 0.995 | 0.94 | 5.1 | 6.3 |
| ACP | 10–500 | 0.993 | 1.04 | 2.9 | 4.5 |
| FLU | 1–500 | 0.991 | 0.29 | 3.5 | 5.7 |
| PA | 1–500 | 0.993 | 0.31 | 4.1 | 6.4 |
| ANT | 1–500 | 0.997 | 0.24 | 5.3 | 7.3 |
| FL | 1–500 | 0.994 | 0.33 | 6.3 | 8.8 |
| PYR | 1–500 | 0.999 | 0.21 | 4.5 | 7.2 |
| BaA | 1–500 | 0.991 | 0.19 | 5.3 | 11.5 |
| CHR | 1–500 | 0.994 | 0.16 | 2.9 | 7.1 |
| BbF | 1–500 | 0.991 | 0.21 | 6.8 | 6.8 |
| BkF | 1–500 | 0.996 | 0.17 | 5.7 | 5.2 |
| BaP | 1–500 | 0.994 | 0.11 | 4.2 | 10.3 |
| IPY | 1–500 | 0.992 | 0.12 | 5.9 | 6.7 |
| DBA | 1–500 | 0.991 | 0.17 | 6.9 | 3.9 |
| BPE | 1–500 | 0.999 | 0.25 | 4.3 | 10.7 |

analytes normalized by coating volume. As for the remaining thirteen analytes, both fibers exhibited affinity. More specifically, compared to the commercial PDMS fiber, the PI-coated fiber showed much higher extraction efficiency toward BaA, CHR, BbF, BkF, BaP, and IPY, exhibiting approximately 5.0- to 28.8-fold higher responses; similar efficiencies were observed for ANT, FL, and PYR. In contrast, lower extraction efficiencies were observed for ANY, ACP, FLU, and PA, with 0.39–0.83-fold responses relative to the PDMS fiber (Fig. 4). This phenomenon may be explained by the abundance of p and π-electrons in its structure. These findings confirm that the PI coating outperforms the PDMS coating in extracting PAHs.

### 3.9. Performance of the SPME-GC/FID method

The performance of the SPME-GC/FID method was evaluated based on linearity, limits of detection (LODs), and repeatability, with results summarized in Table 1. Linearity was assessed using water samples spiked with PAHs across a concentration range of 1–500 $\mu g\ L^{-1}$, analyzed in triplicate. All analytes exhibited excellent linearity, with determination coefficients ($R^2$) exceeding 0.99. The LODs, defined as the lowest concentrations detectable with a signal-to-noise ratio of 3, ranged from 0.11 to 1.23 $\mu g\ L^{-1}$. Repeatability tests with a single PI-coated fiber yielded relative standard deviations (RSDs) below 6.9% over five extractions of a 100 μg per L PAH solution. Fiber-to-fiber variation, evaluated using three PI-coated fibers, showed RSDs below 11.5%. These results confirm the method's sensitivity, reproducibility, and consistent fabrication quality.

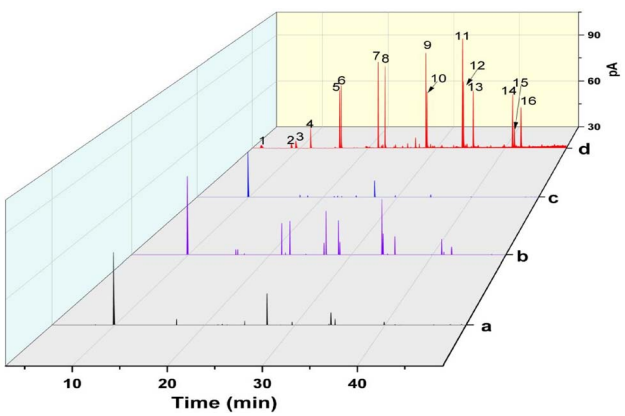


Fig. 5 Chromatograms of (a) a Yellow River water sample, (b) a sewage water sample, (c) a lake water sample, and (d) a standard solution (100 $\mu g\ L^{-1}$).

### 3.10. Sample analysis

The GC/FID method was validated by analyzing fifteen PAHs in three types of environmental water samples: Yellow River water, sewage water, and lake water. The results are presented in Fig. 5 and Table 2. LA, PYR, BkF, and BbF were detected in Yellow River water at concentrations of 2.7, 1.8, 3.9, and 1.1 $\mu g\ L^{-1}$, respectively. In sewage water, FLU, PA, ANT, FL, PYR, BaA, CHR, BbF, BkF, BaP, IPY, DBA, and BPE were identified, with concentrations ranging from 4.5 to 53.5 $\mu g\ L^{-1}$. In lake water, four PAHs (LA, PYR, BkF, and BbF) were detected at concentrations of 3.6, 2.5, 1.1, and 1.4 $\mu g\ L^{-1}$, respectively. To verify the method's accuracy, three different types of real water samples were spiked with 100.0 $\mu g\ L^{-1}$ of PAHs, achieving recoveries ranging from 82.7% to 107.2%. The corresponding chromatograms are shown in Fig. S4–S6.† These findings confirm the reliability and effectiveness of the method for analyzing PAHs in complex water matrices.

Table 2 Analytical results for the determination of PAHs in natural water samples[a]

| Compound | Yellow River water | | | Sewage water | | | Lake water | | |
|---|---|---|---|---|---|---|---|---|---|
| | Concentration (μg $L^{-1}$) | RSD (%, $n = 3$) | Recovery (%) | Concentration (μg $L^{-1}$) | RSD (%, $n = 3$) | Recovery (%) | Concentration (μg $L^{-1}$) | RSD (%, $n = 3$) | Recovery (%) |
| NAP | – | 3.3 | 90.1 | – | 5.5 | 84.7 | – | 4.9 | 82.8 |
| ANY | – | 4.2 | 88.5 | – | 6.2 | 90.4 | – | 5.1 | 106.7 |
| ACP | – | 5.6 | 82.7 | – | 4.8 | 87.2 | – | 6.4 | 92.4 |
| FLU | – | 4.2 | 86.4 | 6.6 | 3.9 | 83.5 | – | 5.1 | 88.4 |
| PA | – | 2.9 | 87.5 | 14.4 | 2.8 | 104.6 | – | 6.2 | 92.4 |
| ANT | – | 5.4 | 90.1 | 15.9 | 4.6 | 86.4 | – | 5.8 | 86.5 |
| FL | 2.7 | 6.1 | 92.3 | 50.1 | 6.2 | 90.4 | 3.6 | 7.1 | 104.6 |
| PYR | 1.8 | 5.3 | 85.2 | 53.5 | 3.9 | 92.4 | 2.5 | 5.3 | 88.3 |
| BaA | 3.9 | 6.1 | 105.3 | 14.0 | 4.8 | 87.8 | 1.1 | 4.9 | 82.6 |
| CHR | – | 5.5 | 92.4 | 6.8 | 5.5 | 91.8 | – | 6.3 | 102.2 |
| BbF | 1.1 | 4.8 | 93.4 | 18.7 | 4.7 | 105.2 | 1.4 | 5.8 | 84.3 |
| BkF | – | 3.7 | 107.2 | 8.6 | 3.9 | 84.7 | – | 4.6 | 94.3 |
| BaP | – | 5.9 | 94.1 | 7.8 | 6.7 | 105.7 | – | 6.1 | 86.7 |
| IPY | – | 6.7 | 86.5 | 7.6 | 5.7 | 102.7 | – | 5.8 | 94.1 |
| DBA | – | 4.9 | 103.5 | 4.6 | 5.7 | 91.8 | – | 4.9 | 83.8 |
| BPE | – | 5.9 | 87.4 | 4.5 | 4.1 | 93.4 | – | 5.8 | 106.4 |

[a] – indicates non-detectable.

## 4. Conclusion

This study introduced a novel supporting material by pulling melted glass onto SSW. The resulting material integrates the mechanical strength of SSW with the chemical properties of glass. Using this approach, robust and flexible PI-coated SPME fibers were fabricated through a simple dipping method. The PI-coated fibers exhibited excellent fiber-to-fiber repeatability, as well as strong solvent resistance, thermal stability, and selectivity for PAHs. These fibers were successfully applied for the extraction of trace PAHs from river, pond, and sewage water samples prior to GC-FID analysis. The method exhibited a wide linear range (1–500 μg $L^{-1}$), low LODs (0.11–1.23 μg $L^{-1}$), and good recoveries (82.7%–107.2%) in real samples, confirming its suitability for environmental analysis. Thus, this PI-coated fiber-based DI-SPME-GC-FID technique provides a sensitive and cost-effective alternative for detecting trace PAHs in complex samples.

## Data availability

The data supporting the findings of this study are available within the article and its ESI.† Additional datasets generated and analyzed during the current study are available from the corresponding author upon reasonable request.

## Conflicts of interest

There are no conflicts to declare.

## Acknowledgements

This work was supported by the National Natural Science Foundation of China (21565005), the Gansu Provincial Science and Technology Plan Project (21YF5GA099), the Gansu Provincial Educational Science and Technology Innovation Project (2021CYZC-41), the Major Scientific & Technological Innovation Project of Gansu University of Political Science and Law (GZF2019XZD03), and the University-level Innovative Research Team of Gansu University of Political Science and Law.

## References

1 K. Woźniczka, P. Konieczyński, A. Plenis, T. Bączek and A. Roszkowska, SPME as a green sample-preparation technique for the monitoring of phytocannabinoids and endocannabinoids in complex matrices, *J. Pharm. Anal.*, 2023, **13**, 1117–1134.
2 W. Zhou and J. Pawliszyn, Perspective on SPME-MS: green and high-performance methods for rapid screening, *Anal. Chim. Acta*, 2024, **1291**, 342244.
3 D. Leszczyńska, A. Hallmann, N. Treder, T. Bączek and A. Roszkowska, Recent advances in the use of SPME for drug analysis in clinical, toxicological, and forensic medicine studies, *Talanta*, 2023, **270**, 125613.
4 D. Su, J. J. He, Y. Z. Zhou, Y. L. Li and H. J. Zhou, Aroma effects of key volatile compounds in Keemun black tea at different grades: HS-SPME-GC-MS, sensory evaluation, and chemometrics, *Food Chem.*, 2022, **373**, 131587.
5 H. Qin, H. Liu, Y. Liu, S. Di, Y. Bao, Y. Zhai and S. Zhu, Recent advances in sample preparation and chromatographic analysis of pharmaceuticals and personal care products in environment, *Trends Anal. Chem.*, 2023, **164**, 117112.
6 A. Khaled, J. R. Belinato and J. Pawliszyn, Rapid and high-throughput screening of multi-residue pharmaceutical drugs in bovine tissue using solid phase microextraction and direct analysis in real time-tandem

mass spectrometry (SPME-DART-MS/MS), *Talanta*, 2020, **217**, 121095.
7 L. Y. Zhao, M. Qin, G. P. Wu, Y. T. Zhou, J. X. Zhu and H. Peng, Quantitative determination of amphetamine-type stimulants in sewage and urine by hybrid monolithic column solid-phase microextraction coupled with UPLC-QTRAP MS/MS, *Talanta*, 2024, **269**, 125437.
8 A. M. Dhabbah, Detection of petrol residues in natural and synthetic textiles before and after burning using SPME and GC-MS, *Aust. J. Forensic Sci.*, 2020, **52**, 194–207.
9 M. Lashgari and Y. Yamini, An overview of the most common lab-made coating materials in solid phase microextraction, *Talanta*, 2019, **191**, 283–306.
10 X. Feng, Y. Li, R. Jing, X. Jiang and M. Tian, Detection of organophosphorous pesticides in soil samples with multiwalled carbon nanotubes coating SPME fiber, *Bull. Environ. Contam. Toxicol.*, 2014, **93**, 769–774.
11 X. Y. Song, J. Chen and Y. P. Shi, Different configurations of carbon nanotubes reinforced solid-phase microextraction techniques and their applications in the environmental analysis, *Trends Anal. Chem.*, 2017, **86**, 263–275.
12 A. Song, J. Wang, G. Lu, Z. Jia, J. Yang and E. Shi, Oxidized multiwalled carbon nanotubes coated fibers for headspace solid-phase microextraction of amphetamine-type stimulants in human urine, *Forensic Sci. Int.*, 2018, **290**, 49–55.
13 N. Xu, Y. Wang, M. Rong, Z. Ye, Z. Deng and X. Chen, Facile preparation and applications of graphitic carbon nitride coating in solid-phase microextraction, *J. Chromatogr. A*, 2014, **1364**, 53–58.
14 J. Chen, J. Zou, J. Zeng, X. Song, J. Ji, Y. Wang, J. Ha and X. Chen, Preparation and evaluation of graphene-coated solid-phase microextraction fiber, *Anal. Chim. Acta*, 2010, **678**, 44–49.
15 A. Piñeiro-García, G. González-Alatorre, F. Tristan, J. C. Fierro-Gonzalez and S. M. Vega-Díaz, Simple preparation of reduced graphene oxide coatings for solid phase micro-extraction (SPME) of furfural to be detected by gas chromatography/mass spectrometry, *Mater. Chem. Phys.*, 2018, **213**, 556–561.
16 X. Zang, Q. Chang, Y. Pang, L. Wang, S. Zhang, C. Wang and Z. Wang, Solid-phase microextraction of eleven organochlorine pesticides from fruit and vegetable samples by a coated fiber with boron nitride modified multiwalled carbon nanotubes, *Food Chem.*, 2021, **359**, 129984.
17 T. D. Ho, A. J. Canestraro and J. L. Anderson, Ionic liquids in solid-phase microextraction: a review, *Anal. Chim. Acta*, 2011, **695**, 18–43.
18 S. Wang, Y. Shi, J. Yu, G. Chen, J. Xu, F. Zhu and G. Ouyang, Mild post-modified metal–organic frameworks applied as solid-phase microextraction coatings for the trace detection of polybrominated biphenyls in human serum, *Microchem. J.*, 2024, **199**, 110001.
19 E. Turiel, J. L. Tadeo and A. Martin-Esteban, Molecularly imprinted polymeric fibers for solid-phase microextraction, *Anal. Chem.*, 2007, **79**, 3099–3104.
20 X. Yang, J. Wang, W. Wang, S. Zhang, C. Wang, J. Zhou and Z. Wang, Solid phase microextraction of polycyclic aromatic hydrocarbons by using an etched stainless-steel fiber coated with a covalent organic framework, *Microchim. Acta*, 2019, **186**, 1–8.
21 Y. Yang, Y. Guo, X. Jia, Q. Zhang, J. Mao, Y. Feng, D. Yin, W. Zhao, Y. Zhang, G. Ouyang and W. Zhang, An ultrastable 2D covalent organic framework coating for headspace solid-phase microextraction of organochlorine pesticides in environmental water, *J. Hazard. Mater.*, 2023, **452**, 131228.
22 M. Mehrabi and V. Vatanpour, Polyimide-based separation membranes for liquid separation: A review on fabrication techniques, applications, and future perspectives, *Mater. Today Chem.*, 2024, **270**, 125613.
23 Y. Ding, H. Hou, Y. Zhao, Z. Zhu and H. Fong, Electrospun polyimide nanofibers and their applications, *Prog. Polym. Sci.*, 2016, **61**, 67–103.
24 K. Hu, J. Cheng, B. Lu, W. Zhao, C. Dong, H. Yang, Y. Huang and S. Zhang, Magnetic mesoporous polyimide composite for efficient extraction of Rhodamine B in food samples, *J. Sep. Sci.*, 2019, **42**, 2023–2031.
25 C. R. Gautreaux, J. R. Pratt and T. L. St Clair, A study of crystalline transitions in a thermoplastic polyimide, *J. Polym. Sci., Part B:Polym. Phys.*, 1992, **30**, 71–82.
26 T. Brock, D. C. Sherrington and J. Swindell, Synthesis and characterisation of porous particulate polyimides, *J. Mater. Chem.*, 1994, **4**, 229–236.
27 Y. Du, X. Yan, Y. Chen, Y. Wu, Q. Qiu, Y. Li and D. Wu, Magnetic polyimide nanosheet microspheres for trace analysis of estrogens in aqueous samples by magnetic solid-phase extraction-gas chromatography–mass spectrometry, *J. Chromatogr. A*, 2022, **1675**, 463184.
28 K. Hu, J. Qiao, W. Zhu, X. Chen and C. Dong, Magnetic naphthalene-based polyimide polymer for extraction of Sudan dyes in chili sauce, *Microchem. J.*, 2019, **149**, 104073.
29 A. Mehdinia, H. Haddad and S. Mozaffari, Polyimide-coated magnetic nanoparticles as a sorbent in the solid-phase extraction of polycyclic aromatic hydrocarbons in seawater samples, *J. Sep. Sci.*, 2016, **39**, 3418–3427.
30 L. Wang, X. Yan, X. Chen, Y. Li and D. Wu, Magnetic polyimide nanocomposite for analysis of parabens in cooking wine by magnetic solid-phase extraction coupled with gas chromatography–Mass spectrometry, *J. Chromatogr. A*, 2024, **1720**, 464814.
31 T. H. Ding, H. H. Lin and C. W. Whang, Determination of chromium (III) in water by solid-phase microextraction with a polyimide-coated fiber and gas chromatography-flame photometric detection, *J. Chromatogr. A*, 2005, **1062**, 49–55.
32 A. K. Haritash and C. P. Kaushik, Biodegradation aspects of polycyclic aromatic hydrocarbons (PAHs): a review, *J. Hazard. Mater.*, 2009, **169**, 1–15.
33 G. W. Vandergrift, E. T. Krogh and C. G. Gill, Direct, isomer-specific quantitation of polycyclic aromatic hydrocarbons in soils using membrane introduction mass spectrometry and chemical ionization, *Anal. Chem.*, 2020, **92**, 15480–15488.

34 S. Gan, E. V. Lau and H. K. Ng, Remediation of soils contaminated with polycyclic aromatic hydrocarbons (PAHs), *J. Hazard. Mater.*, 2009, **172**, 532–549.
35 X. Wang, Z. Zhang, J. Ru, P. Huang, Y. Ma, J. Zhang, X. Du and X. Lu, Hierarchical porous MOFs@ COFs-based molecular trap solid-phase microextraction for efficient capture of PAHs and adsorption mechanisms, *Sep. Purif. Technol.*, 2024, **328**, 125041.
36 R. Zakerian and S. Bahar, Electrochemical exfoliation of pencil graphite for preparation of graphene coating as a new versatile SPME fiber for determination of polycyclic aromatic hydrocarbons by gas chromatography, *Microchim. Acta*, 2019, **186**, 1–7.
37 S. Zhang, Z. Du and G. Li, Layer-by-layer fabrication of chemical-bonded graphene coating for solid-phase microextraction, *Anal. Chem.*, 2011, **8**, 7531–7541.
38 Y. Zhao, K. Hu, C. Yang, X. Liu, L. Li, Z. Li, P. Wang, Z. Zhang and S. Zhang, Covalent organic framework@ Ti3C2Tx composite as solid phase microextraction coating for the determination of polycyclic aromatic hydrocarbons in honey samples, *Anal. Chim. Acta*, 2023, **1237**, 340581.